PHYSICAL REVIEW A VOLUME 42, NUMBER 4 15 AUGUST 1990

Neutrally stable fronts of slow convective traveling waves

Paul Kolodner
AT&T Bell Laboratories, Murray Hill, New Jersey 07974
(Received 10 May 1990)

I report experiments on a new confined state of convection, in which slow traveling rolls exist in a region of arbitrary length in a rectangular cell, separated from the rest by a front that can be motionless. In contrast to other "confined" states observed in this system, the convective state behind this front is well understood on the basis of the Navier-Stokes equations. This suggests that the stability of the front can be posed as a separate theoretical problem.

Traveling-wave (TW) convection in binary-fluid mixtures exhibits a strong propensity to form "confined states," in which TW's are observed in isolated regions surrounded by motionless fluid.[1-3] One such state, first seen in an annular geometry at a separation ratio $\psi=-0.25$, consists of patches of apparently arbitrary length,[2] within which rolls travel much faster than the nonlinear TW's which fill the cell at the same Rayleigh number r. I refer to such states as "fast confined states" (FCS's). The fronts that separate the convecting patches from the surrounding quiescent fluid are "locked" in space over a small range of r inside the hysteresis loop between the linear onset r_{co} and the saddle-node point $r_s < r_{co}$. For smaller $|\psi|$, other confined states have been observed.[1,3] While some of these observations resemble solutions of model equations,[4] the fact remains that in none of these cases is there a full understanding of the convecting state inside the confined region. This is especially frustrating in the case of the FCS's in Ref. 2 because their extent can be quite large. Thus, it seems reasonable to expect that the convecting state observed inside the confined patches could exist in an infinite system with no confinement, and the theoretical problem of explaining such an extended state ought to be comparatively simple: one searches for a branch of "fast" solutions to the Navier-Stokes equations as well as the usual "slow" branch. Once this is solved, the stability of the confining fronts might then be approached separately.

In this paper, I present observations of a new confined state, for which this separation of the front-stability problem from the extended-convective-state problem is already partly solved. In these states, slow TW's are observed in a region that is bounded on one side by a cell wall and on the other by a motionless front in the interior of the cell. These "slow" confined states (SCS's) can fill an arbitrary fraction of the cell. The convective state behind the front is shown to be the same as the nonlinear TW state which fills the cell at the same r. Unlike the FCS's, this slow state is well understood in an infinite system on the basis of both numerical integrations of the Navier-Stokes equations[5] and a perturbative expansion in powers of ψ.[6] I present observations of the behavior of the confining front and of the influence of lateral end walls on the convective state. It seems reasonable to expect that both of these finite-size effects can be explained in the context of the theory of the extended TW state.

The apparatus has been described previously.[7,8] The cell is a rectangular channel in a plastic frame of thickness $d=0.348$ cm and width $3.0d$. One end wall is a plug that can be moved to change the cell length Γd from $\Gamma\sim 11$ to ~ 21. The bottom plate of the cell is a rhodium-plated copper mirror which is heated from below. The top plate is a sapphire window that is cooled from above by circulating, temperature-regulated water. The fractional long-term stability of temperature difference applied across the cell ranges from 3 to 6×10^{-5}. The flow pattern is visualized from above by shadowgraphy. A change-coupled-device (CCD) camera views the entire two-dimensional image of the flow, and a photomultiplier records the light intensity at a single spatial point. The convective patterns are essentially one dimensional, consisting of wave fronts which are parallel to the short side of the cell and which propagate parallel to the long side. Thus, the CCD camera records the light intensity in 200 pixels which are arrayed parallel to the long side of the cell, along its centerline. Complex demodulation of these multipoint time series is used to separate the oppositely propagating components of the TW pattern and to compute their spatial wave-number profiles.[8] Demodulation in the time domain alone is used to compute the spatial profiles of the amplitudes in states of unidirectional waves, so as to avoid the smoothing inherent in spatial demodulation.

The fluid is a 4.40-wt.% solution of ethanol in water. With a top-plate temperature of 20.0 °C (10.0 °C) and an applied temperature difference of 3.9 °C (7.9 °C), the separation ratio $\psi=-0.240$ (-0.408), the Prandtl number $P=9.03$ (11.61), and the Lewis number $L=0.0076$ (0.0062).[9] The cell length was $\Gamma=19.01$ (20.22). Similar results were obtained in both cases. In this paper, lengths are scaled by the cell height d, velocities are scaled by κ/d, where κ is the thermal diffusivity of the fluid, and I quote values of the reduced Rayleigh number r, which is the ratio of the actual Rayleigh number R to the critical Rayleigh number $R_c=1707.8$ calculated for the onset of steady convection in an infinite layer of a pure fluid with the same thermal properties as the mixture.

The experiments are begun by raising r a few percent above the onset $r_{co}=1.3823$ (1.7457) measured for the linear TW instability at $\psi=-0.240$ (-0.408).[7,8] As observed previously in experiments on two-dimensional TW patterns in much wider cells,[10] the nonlinear evolution of

the instability consists of a "spatial collapse," in which convection becomes confined to a small patch in the center of the cell. If r is held above r_{co}, this patch expands to fill the entire cell with slow, one-dimensional TW's. However, this can be avoided by reducing r during this phase. If r is dropped to within a narrow band just above the saddle-node point, then the confined patch can be maintained in the center of the cell, with properties which vary only slowly in time. An example is shown in the bottom of Fig. 1. The rolls in this small patch exhibit a relatively high oscillation frequency $\omega_f = 5.19$, and different protocols can be used to produce confined patches of any length and with either roll-propagation direction. This state is the fast confined state of Ref. 2.

In contrast to the observations in an annulus in Ref. 2, the location of the FCS in Fig. 1 is not stable. Instead, as illustrated in the middle of Fig. 1, the fast confined patch is always observed to drift slowly ($v_{\text{drift}} \sim -0.04$) in the direction opposite to the roll propagation. It is not known why this happens, but it inevitably leads (Fig. 1, top) to the production of a confined patch of rolls whose trailing edge (defined as the boundary of the confined region from which rolls originate, as opposed to opposite *leading* edge) coincides with the wall of the cell. As shown in Fig. 2, the oscillation frequency drops when the trailing edge encounters the wall. The state in the top of Fig. 1 is a time-independent slow confined state.

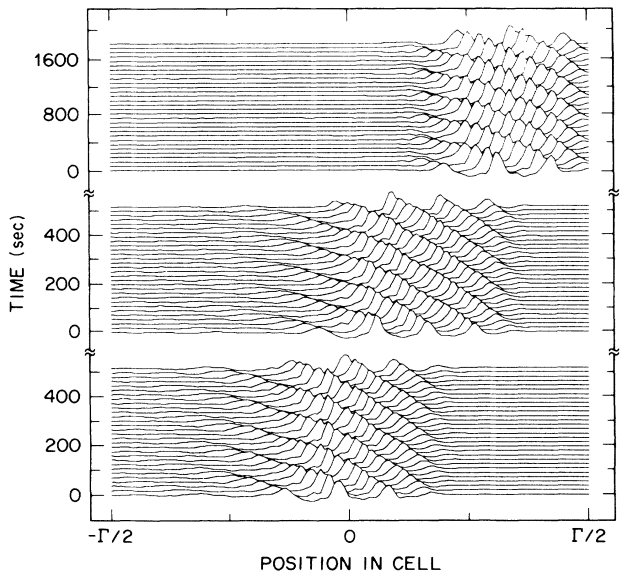

FIG. 1. Three hidden-line plots illustrate the evolution, for $\psi = -0.240$, of a fast confined state in the center of the cell into a slow confined state whose trailing edge coincides with the end wall of the cell. In each, the shadowgraph image intensity is plotted as a function of position in the cell at successive instants in time. Bottom: small confined patch of fast left-going rolls at $r = 1.2669$. Sample time 18 s. Shortly after this observation, r was decreased to 1.2634. Middle: 3.1 h later, the patch has moved to the right side with little change in envelope shape or wave speed. Top: 6.5 h later, the patch of rolls has moved against the end wall of the cell, and the wave speed has dropped by a factor 3.5 (sample time 63 s). This "slow confined state" is now stable.

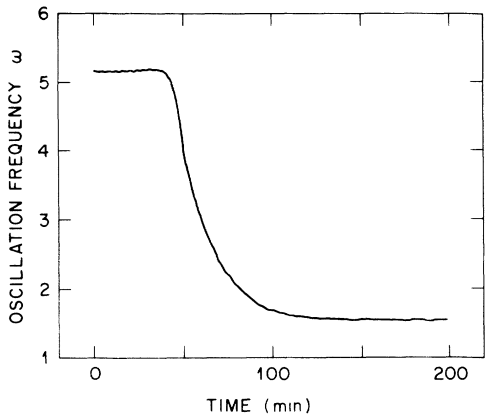

FIG. 2. The oscillation frequency is plotted as a function of time during an evolution like the one shown in Fig. 1, with $\psi = -0.240$ and $r = 1.2734$. Initially, the convective structure consists of an isolated patch of rolls in the center of the cell, and the frequency is high ($\omega_f = 5.19$). As the trailing edge of the patch moves near the wall, the frequency drops to $\omega_s = 1.50$. For comparison, the observed frequency of the linear instability which triggers the onset of convection at $r_{co} = 1.3823$ is $\omega_0 = 11.84$.

There are also important differences between these observations and the confined-state evolution that was described for $\psi \sim -0.1$ in Ref. 1. For smaller $|\psi|$, the confined states are observed only above onset, and it is their *leading edge* which coincides with the cell wall. The latter feature has been shown[4] to be a consequence of the convectively unstable nature of the Ginzburg-Landau equation which models this system for small $|\psi|$. The confined states in Ref. 1 also have a fixed shape and size, and this too is a result obtained with the Ginzburg-Landau model. By contrast, the shape of the SCS observed here is not fixed. If r is increased, its leading edge expands slowly into the cell. If r is then decreased sufficiently, the front will recede again towards the cell wall. In this way, a SCS of any length can be produced.

Isolated spatial regions of slow TW's were also reported in an annular geometry in Ref. 2. There, however, the trailing edge was unstable to fast rolls, so that the slow TW's were always replaced by fast confined states. When the trailing edge touches a wall, however, this instability is suppressed, and the behavior of the leading edge can be studied for long times. At $\psi = -0.408$, the motion of this front always proceeds at a constant velocity v_{fr} long after a change in r. As shown in Fig. 3(a), v_{fr} is a linear function of r, with slope $dv_{\text{fr}}/dr = 1.00 \pm 0.02$. There is no evidence for a band of r over which the front position is locked, as was seen for FCS's in Ref. 2. At $\psi = -0.240$, the front motion is more complicated. The fronts usually slow down long after a change in r. By fitting the front position to a function of the form $x(t) = v_{\text{fr}} t (1 - t^2/t_0^2)^{-1/2}$, an initial velocity can be extracted from such observations. The variation of v_{fr} with r is again roughly linear at this ψ, with slope $dv_{\text{fr}}/dr = 1.9 \pm 0.2$.

v_{fr} vanishes at a unique Rayleigh number $r_v = 1.2630 \pm 0.0002$ (1.4049 ± 0.0001) for $\psi = -0.240 (-0.408)$,

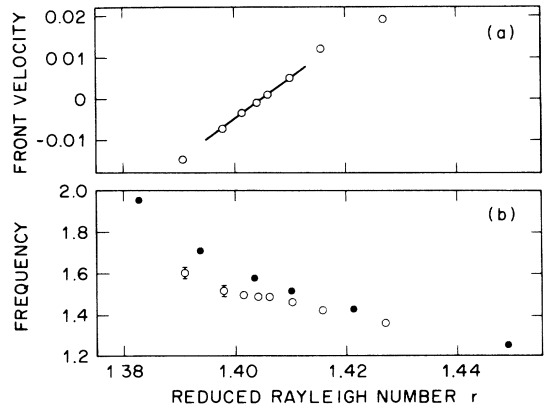

FIG. 3. (a) Front velocity v_{fr} vs reduced Rayleigh number r for $\psi = -0.408$. Near $r_v = 1.4049$, the relationship is linear, with no evidence of locked fronts. The least-squares-fit line has a slope $dv_{fr}/dr = 1.00 \pm 0.02$. (b) Oscillation frequency vs r for the full-cell state (solid symbols) and the SCS (open symbols), for $\psi = -0.408$. Above r_v, the expanding SCS has a frequency almost identical to that in the full-cell state. Below r_v, the frequency is noticeably lower and is unstable in time, leading to large error bars.

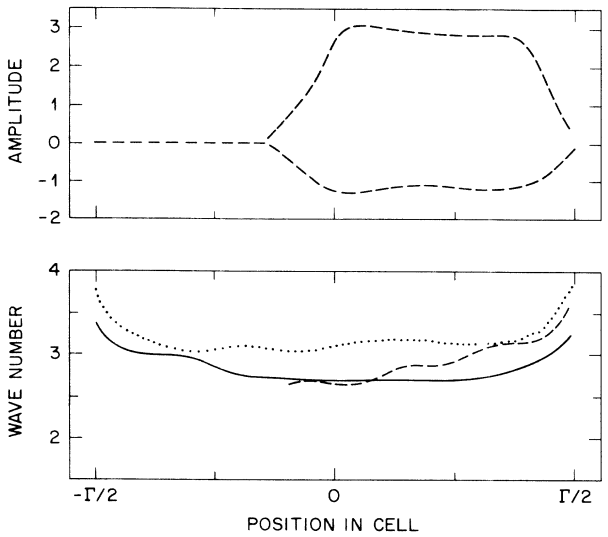

FIG. 4. Top: the spatial profile of the amplitude of left-going rolls in a SCS with $\psi = -0.240$ is shown at $r = 1.2634$. The trailing edge for this state is at the right end wall of the cell. This profile was made by overlaying plots of the image intensity made at different times and tracing the envelope of the TW, so as to avoid the smoothing inherent in spatial demodulation. Bottom: the spatial profile of the wave number as computed using complex demodulation is shown for various states. Dashed curve: profile of the left wave number for the SCS in the top of the figure. Solid curve: wave number for a right-going full-cell state at the same value of r. Here, the "trailing-edge end wall" refers to the left wall of the cell. Dotted curve: left wave number k_{lin} for linear counterpropagating waves seen exactly at onset. In both nonlinear states, the wave number in the center of the cell is much lower than k_{lin}.

just above the saddle-node point at $r_s = 1.254 \pm 0.004$ (1.339 ± 0.008). At both values of ψ, I have produced *neutrally stable* SCS's, in which the front was motionless for weeks, by setting $r = r_v$. The magnitude of the velocities in Fig. 3(a) can be appreciated by noting that the TW themselves have a much higher propagation velocity at $r = r_v$; i.e., $v_{TW} = 0.554 \pm 0.009$, a value which is identical for both values of ψ.

The convective state behind the front in a sufficiently large SCS is the same as the full-cell state seen at the same value of r. This is shown in Figs. 3(b) and 4. In the top of Fig. 4 is the spatial profile of the amplitude of a SCS of left-going rolls at $r = 1.2634 \sim r_v$. The full-cell state at this r has the same amplitude and shows a similar decrease in amplitude near the trailing-edge end wall. In both states, complex demodulation yields a very weak oppositely propagating wave component with an incoherent spatial phase, a signature consistent with zero amplitude. The dashed curve in the bottom of Fig. 4 shows the wave number in this SCS, and the solid curve shows the wave-number profile for a right-going full-cell state in another run at the same r. In both states, the confined-state wave number drops from a slightly elevated value near the trailing-edge end wall to a value $k_s = 2.7$ in the center of the cell that is markedly lower than the wave number $k_{lin} \sim \pi$ of linear waves seen exactly at onset (dotted curve). The length of the region over which the wave number changes is about nine times the cell height. The wave-number profiles of SCS and full-cell states which propagate in the same direction exhibit the same shape near the trailing-edge end wall. However, this shape is slightly different for left- and right-going waves, because of a slight left-right asymmetry in the apparatus which appears to be due to optical distortions.

Figure 3(b) shows the dependence of the oscillation frequency on r for the full-cell state (solid circles) and the SCS (open circles) for $\psi = -0.408$. The full-cell frequency dependence is quite similar to theoretical predictions[5,6] and to recent measurements in an annulus.[11] Above r_v, the frequencies of the two states differ by only 1–2%, and both settle to a constant value within about one vertical concentration diffusion time following a change in r. Below r_v, the rolls in the SCS are slower than those in the full-cell state, and, as represented by the error bars, the SCS frequency continues to drift long after changes in r. With the assertion that the wave number at the front has an effect on the oscillation frequency measured behind it, these features can be understood with reference to the wave-number profile of the SCS shown in Fig. 4. Sufficiently long after r has been increased above r_v, the leading edge of the SCS will have moved into the region in the center of the cell, where the wave number is constant. Further propagation of the front has no effect on the state behind it. At long times after r has been reduced below r_v, however, the front will inevitably be moving through the region near the end wall where the wave number is a strong function of position, causing a continual change in the oscillation frequency with time. A SCS of sufficient length appears identical to the state that would be seen in a semi-infinite system bounded only by a trailing-edge end wall.

In this paper, I have identified a new confined state of traveling-wave convection in which slow TW's propagate behind a leading-edge front which can be made neutrally stable. The significance of this observation is that these TW's lie on a branch of solutions to the Navier-Stokes equations which is well understood in an unbounded, one-dimensional geometry. Thus the first step in understanding the stability of this front has already been taken. Perhaps one clue in this understanding is that the front velocity vanishes when the wave speed has the same particular value at two different values of separation ratio. These experiments also reveal that the nature of TW's that propagate away from an end wall is effected by that wall only within a distance of about nine times the cell height. The influence of a single boundary in a semi-infinite system also ought to be one of the first questions answered by a theory of boundary effects on slow TW convection.

I thank P. C. Hohenberg and C. M. Surko for useful discussions and H. Williams for technical assistance.

[1]E. Moses, J. Fineberg, and V. Steinberg, Phys. Rev. A **35**, 2757 (1987); R. Heinrichs, G. Ahlers, and D. S. Cannell, *ibid.* **35**, 2761 (1987).

[2]P. Kolodner, D. Bensimon, and C. M. Surko, Phys. Rev. Lett. **60**, 1723 (1988); D. Bensimon, P. Kolodner, C. M. Surko, H. L. Williams, and V. Croquette, J. Fluid Mech. **217**, 441 (1990).

[3]J. J. Niemela, G. Ahlers, and D. S. Cannell, Phys. Rev. Lett. **64**, 1365 (1990).

[4]M. C. Cross, Phys. Rev. Lett. **57**, 2935 (1986).

[5]W. Barten, M. Lücke, W. Hort, and M. Kamps, Phys. Rev. Lett. **63**, 376 (1989).

[6]D. Bensimon, A. Pumir, and B. I. Shraiman, J. Phys. (Paris) **50**, 3089 (1989).

[7]P. Kolodner, C. M. Surko, and H. Williams, Physica D **37**, 319 (1989).

[8]P. Kolodner and H. Williams, in *Proceedings of the NATO Advanced Research Workshop on Nonlinear Evolution of Spatio-Temporal Structures in Dissipative Systems,* edited by F. H. Busse and L. Kramer, NATO Advanced Study Institute, Series B2, Vol. 225 (Plenum, New York, 1990), pp. 73–91.

[9]P. Kolodner, H. Williams, and C. Moe, J. Chem. Phys. **88**, 6512 (1988).

[10]P. Kolodner, A. Passner, H. L. Williams, and C. M. Surko, Nucl. Phys. (Proc. Suppl.) **B2**, 97 (1987).

[11]D. R. Ohlsen, S. Y. Yamamoto, C. M. Surko, and P. Kolodner (unpublished).